PHYSICAL REVIEW B VOLUME 33, NUMBER 8 15 APRIL 1986

Optical reflectivity and electronic structure of layered cadmium halides

I. Pollini
Dipartimento di Fisica, Università degli Studi di Milano and Gruppo Nazionale Struttura della Materia
del Consiglio Nazionale delle Ricerche, via Celoria 16, I-20133 Milano, Italy
and Laboratoire d'Utilisation du Rayonnement Electromagnétique, Université de Paris-Sud, F-91405 Orsay, France

J. Thomas
Laboratoire de Spectroscopie, Université de Rennes I, F-35042 Rennes, France
and Laboratoire d'Utilisation du Rayonnement Electromagnétique, Université de Paris-Sud, F-91405 Orsay, France

R. Coehoorn and C. Haas
Laboratory of Inorganic Chemistry, Materials Science Center of the University of Groningen,
Nÿenborgh 16, 9747 AG Groningen, The Netherlands
(Received 3 December 1985)

The dielectric function $\hat{\varepsilon}(E)$, the energy loss function $-\mathrm{Im}[1/\hat{\varepsilon}(E)]$, and plots of $n_{\mathrm{eff}}(E)$ and $\varepsilon_{\mathrm{eff}}(E)$ have been obtained in the region 2—31 eV by Kramers-Kronig analysis of near-normal-incidence reflectance spectra of single crystals of $CdCl_2$, $CdBr_2$, and CdI_2. The results have been described in terms of interband transitions and plasma oscillations. The low-temperature spectra of the materials reveal the presence of strong exciton structures. Plasma resonance effects have been identified in the high-energy region (15—22 eV). The optical spectra of CdX_2 ($X=$Cl, Br, I) were analyzed in terms of the calculated band structures of $CdCl_2$ and CdI_2. In CdI_2 the smallest energy gap for forbidden (phonon-assisted) direct transitions (at the L point of the Brillouin zone) is 3.8 eV (300 K), while the gap for allowed direct transitions (at Γ) is 4.3 eV (30 K). The fundamental energy gap in $CdCl_2$ and $CdBr_2$ is observed at 6.4 and 5.4 eV, respectively, and corresponds to allowed direct transitions at Γ. The observed excitons X_0, X_1, and X_2 are associated with allowed direct transitions between the halogen np valence band and the Cd $5s$ conduction band. The excitons A, B, and C are due to transitions of electrons from the halogen valence band to the Cd $5p$ conduction band.

I. INTRODUCTION

Cadmium halides are ionic layered materials, exhibiting a strong structural anisotropy, which favors cleavage along their basal planes. The basic structure of these materials consists of layers of cadmium atoms sandwiched between two sheets of halogen atoms; the cadmium atoms being octahedrally coordinated. Because of the weak binding between the layers, different stacking sequences represent only small differences in total energy and in this way several sequences are possible. In the case of CdI_2, for example, over 160 polytypes have been reported.[1] Especially on CdI_2, a large amount of research has been carried out on optical absorption and reflection,[2–11] and on the photoconductivity.[12–14] In addition, the luminescence of the cadmium halides has been studied extensively.[11,15–23] The photolysis of CdI_2 (and PbI_2) is of interest for nonsilver halide photography.[24–26] Several authors have carried out band-structure calculations for CdI.[27–30] Electron-energy-loss (EEL) measurements have been carried out on polycrystalline films.[31]

Both luminescence and photolysis depend on the creation of excitons as a first result of the interaction with light. Therefore, a more detailed knowledge about the nature of the excitonic states in these layered halides is of interest. However, despite the numerous studies, the optical and electronic properties of these compounds are still not well known over a large energy range. This is the reason why we decided to study, anew, the optical properties of the cadmium halides at low temperature over an energy range as large as 2—31 eV,[32] in order to compare the results with recent band-structure calculations.[30] We also report a calculation of the band structure of $CdCl_2$.

After a short description of the methods used for the growth of crystals (Sec. II) we analyze in Sec. III the obtained reflectance spectra and the optical constants. In Sec. IV we discuss the observed structures in terms of excitons, band-to-band transitions and collective excitations (plasmons), using the available band-structure calculations as an aid. The conclusions are summarized in Sec. V.

II. CRYSTAL GROWTH AND STRUCTURE

Cadmium iodide was prepared from the elements in a way analogous to the preparation of nickel iodide,[33] starting from Koch Light 6N cadmium at a temperature of 320—400 °C. Cadmium chloride and bromide were prepared starting from commercially obtained pro-analyse quality hydrates. After drying, the raw materials were purified via sublimation at about 500 °C. The growth of crystals was carried out in two ways; (i) by a Bridgman method, and (ii) by vapor transport in a sealed ampoule, as described by Levy.[34] Besides, $CdCl_2$ and $CdBr_2$ were also prepared by the flow system method by means of the reaction between Cd and HCl, or the direct bromination of cadmium, at temperatures around 450 °C. The obtained crystals are colorless, pearly flakes, slightly hygroscopic. The crystals obtained with different methods have all been used for reflectance measurements, in general all with good results. The crystals obtained from the vapor phase gave the best optical spectra, with well-resolved spectra features.

Cadmium chloride and cadmium bromide crystallize in the $CdCl_2$ structure with a cubic close packing of the halide ions. The most common polytype of CdI_2, essentially the only form grown from the melt and vapor phase,[35] is the $4H$ type $(ABCB)_n$, the simplest mixed form of stacking, consisting of alternating hexagonal and cubic packed anion layers. For the Bridgman grown CdI_2 crystals the single occurrence of the hexagonal $4H$ form was established using the Debye-Scherrer technique. Polytypism has been observed also in $CdBr_2$,[36] but to a far lesser extent than in the case of CdI_2. The most common type and the only type emerging from the melt or vapor phase, is the $CdCl_2$-type structure ($6R$ form). Polytypism has not been reported for $CdCl_2$.

III. EXPERIMENTAL RESULTS

The experimental optical techniques for measuring reflectance spectra of crystals using synchrotron radiation have been described previously.[33,37] Figure 1 shows the reflectance spectra for nearly normal incidence (20°) on cleaved surfaces of the cadmium halide crystals. These spectra correspond (approximately) to a polarization with the electric vector of the light perpendicular to the crystallographic c axis ($\mathbf{E}\perp c$). The spectra were measured at low temperature (30 K) in the whole spectral region 2–31 eV. Figure 2 illustrates the region richer in structure (2–11 eV) in more detail. The three spectra are very similar, and show well-resolved structures in comparison with the spectra observed for evaporated films.[4] The observed peaks and structures can be divided into three groups. The first one contains a series of peaks X_0 to S around the fundamental optical gap (X'_1 shoulder in Fig. 2). The second group, peaks A–C, displays very sharp lines, suggesting a strong exciton mechanism in an energy region about 3 eV above the optical gap. At higher energies, broad maxima are observed (E,F,G) and beyond the band G the reflectance decreases smoothly, as is usually found in ionic and partially ionic crystals, entering the region of plasma effects.

From Fig. 2 we see that in $CdCl_2$ the low-energy part of the spectrum shows a strong peak X_1, followed at higher energy by strong peaks A and B. The peak B is apparently double (B,B') with an energy splitting below or equal to 0.1 eV. The labels B, B', and C in Fig. 2 indicate that this strong structure might also consist of three overlapping peaks, as suggested by comparison with the spectra of $CdBr_2$ and CdI_2. In $CdBr_2$ the low-energy structures X_1 and X_2 have a resonance-like shape; the higher-energy structures A, B, B', and C are well separated, with half widths less than 0.05 eV. The energy separation between peaks X_1 and X_2 is about 0.48 eV. In CdI_2 we observe a strong peak X_2, separated from X_1 by 0.95 eV, a very narrow line A (half width 0.01–0.02 eV), and a further splitting of peaks B (B,B',B'') and C (C,C'). The observed spectra of $CdCl_2$ and $CdBr_2$ are in good agreement with data reported by Kondo *et al.*,[8,10] but our spectra show some additional structure and extend to higher energies.

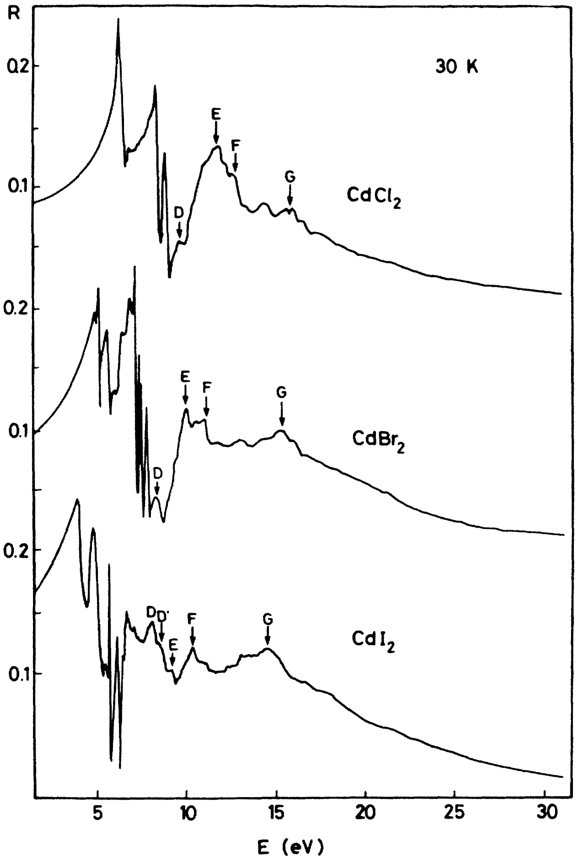

FIG. 1. Reflectivity spectra of $CdCl_2$, $CdBr_2$, and CdI_2 single crystals at 30 K.

A final comment concerns the comparison of the low temperature (30 K) spectra displayed in Figs. 1 and 2 with the room-temperature data we obtained. The broad maxima D, E, F, and G do not change appreciably on cooling to 30 K. On the other hand, the excitonic structures, especially in $CdBr_2$ and CdI_2, present peaks (resonances) and antiresonances which sharpen considerably at low temperature. The sharp antiresonances caused by interference with the scattering continuum are typical of a class of anisotropic, almost two-dimensional, crystals of ionic character.[38]

In Fig. 3 we have represented the real and imaginary parts of the complex dielectric constant $\hat{\varepsilon}=\varepsilon_1+i\varepsilon_2$ as a function of the energy, as deduced from a Kramers-Kronig analysis of the reflectance data. In Fig. 4 we show the comparison between the optical energy-loss function $-\mathrm{Im}(\hat{\varepsilon}^{-1})$, obtained via Kramers-Kronig transforms from the reflectance data, and the electron-energy-loss

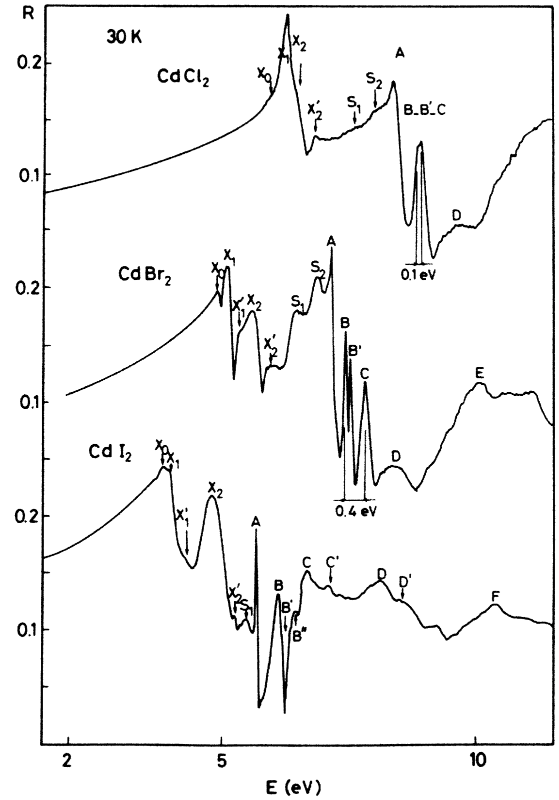

FIG. 2. Details of the reflectivity spectra in the excitonic region around the optical energy gap E_G. Two groups of excitons are observed: The first group (X_0,X_1,X_2) is near E_G, the second one (A,B,C) is above E_G.

functions for $CdCl_2$, $CdBr_2$, and CdI_2 at low scattering angles. With the exception of CdI_2, this comparison shows that the electron-energy-loss data for polycrystalline films obtained by Bringans and Liang[31] are in rather good agreement with our optical data for single crystals. We remark that the sharp electronic features observed in the optical spectra below 10 eV, are less pronounced in the electron-energy-loss data because of the much lower energy resolution of this latter method.

The main feature of the energy-loss spectra are the broad plasmon peaks, which occur in the optical spectra at about 21 eV for all three halides, and are observed in the electron-energy-loss spectra between 16.3 and 17.3 eV. These values are compared in Table I with calculated values of the plasmon energy $\hbar\omega_p$. In the first column of Table I we give the values $\hbar\omega_{p0}$, calculated from the free-electron equation

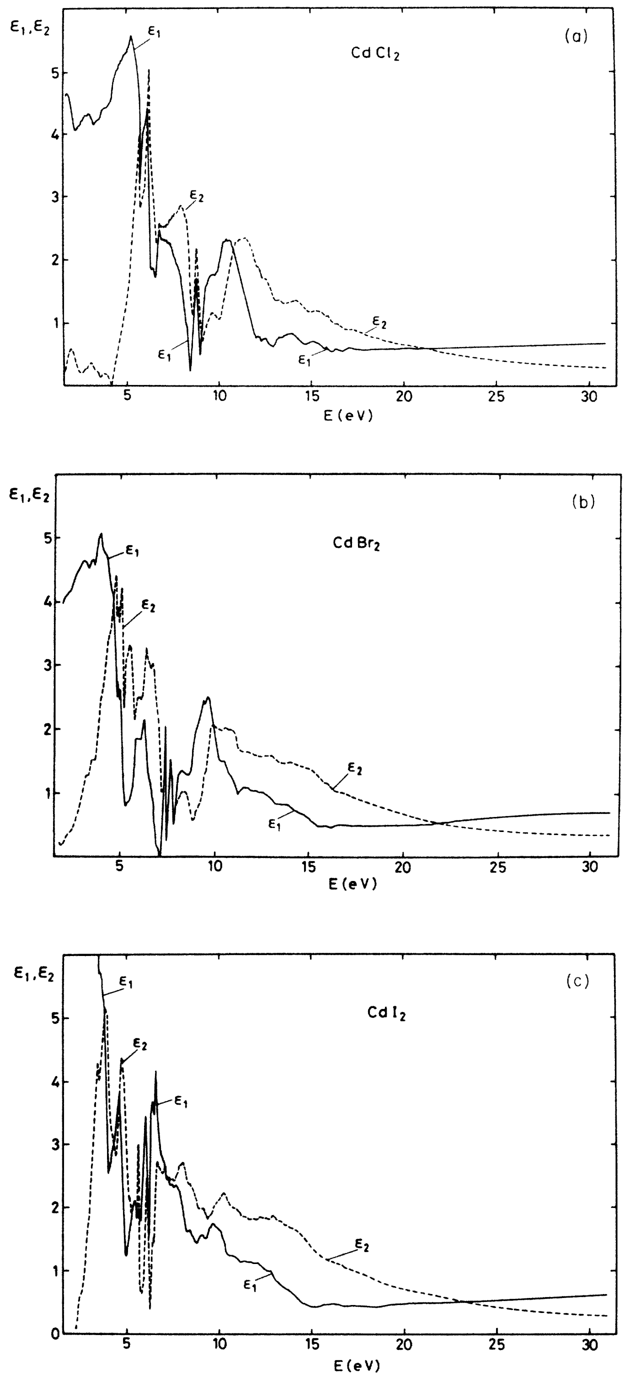

FIG. 3. Spectra of the real and imaginary parts of the complex dielectric constant $\tilde{\varepsilon}(E)=\varepsilon_1(E)+i\varepsilon_2(E)$, calculated by a Kramers-Kronig analysis: (a) $CdCl_2$; (b) $CdBr_2$; (c) CdI_2.

TABLE I. Comparison of plasma frequencies (eV) as given by the free-electron value $\hbar\omega_{p0}$; the Horie relation $\hbar\omega_p$; the standard plasma dispersion relation $\varepsilon_1(\omega_p)\simeq 0$; the maximum of the energy-loss function from optical data $-\mathrm{Im}(1/\tilde{\varepsilon})_{\max}$ and electron energy loss (EEL).

	$\hbar\omega_{p0}$	$\hbar\omega_p$	$\varepsilon_1(\omega_p)\simeq 0$	$-\mathrm{Im}(\tilde{\varepsilon}^{-1})_{\max}$	EEL
$CdCl_2$	14.8	16.1	17.0	20.6	17.3
$CdBr_2$	14.7	15.7	16.0	21.0	17.0
CdI_2	12.4	13.1	15.0	21.7	16.3

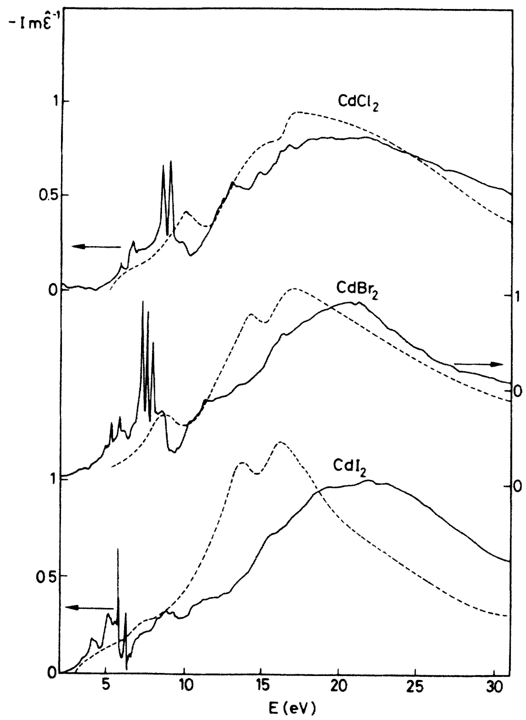

FIG. 4. Comparison between the energy-loss function obtained from reflectivity at 30 K (solid line) and electron-energy-loss data obtained by Bringans and Liang (Ref. 31) (dashed line).

$$\omega_{p0}^2=\frac{4\pi n e^2}{m} \tag{1}$$

with $n=6$ electron per halide ion; secondly we give values of $\hbar^{\omega}_{p0}$ obtained from Horie's formula[39]

$$\omega_p=\omega_{p0}[1+(E_G/\hbar_{p0})^2]^{1/2}\ , \tag{2}$$

where E_G is the energy gap between valence and conduction bands. Finally we give the values of $\hbar\omega_p$, estimated from the minimum of $\varepsilon_1(E)$, i.e., the best approximation to the relation $\varepsilon_1(\hbar\omega_p)=0$. The values calculated with Horie's equation are rather close to the values obtained experimentally, i.e., from the minima of $\varepsilon_1(E)$ and from EEL data. We remark that it is difficult to determine the position of the maxima accurately for these broad structures.

In Fig. 5 we have shown plots of $n_{\rm eff}(E)$, the effective number of electrons per CdX_2 molecule contributing to the optical absorption at photon energy E, and $\varepsilon_{\rm eff}(E)$, the effective dielectric constant

$$n_{\rm eff}(E)=\frac{2m\varepsilon_0 V}{\pi\hbar^2}\int_2^E E'\varepsilon_2(E')dE'\ , \tag{3}$$

$$\varepsilon_{\rm eff}(E)=1+\frac{2}{\pi}\int_2^E\frac{\varepsilon_2(E')}{E'}dE'\ . \tag{4}$$

As a lower bound of the integration we take a photon energy of 2 eV, below which virtually no optical absorption due to electronic transitions occurs in the cadmium halides. At higher energy $n_{\rm eff}$ is expected to saturate at a value of 22, corresponding to 10 valence electrons of the Cd ion and 12 electrons of the halogen ions of each CdX_2 molecule. The crystal volumes (unit cells) employed for the calculation of $n_{\rm eff}$ are $V=74.84$ Å^3 (CdCl$_2$), $V=84.29$ Å^3 (CdBr$_2$), and $V=106.49$ Å^3 (CdI$_2$). Around 7 (CdI$_2$), 9 (CdBr$_2$), and 10.5 eV (CdCl$_2$) $n_{\rm eff}$ begins to increase and reaches the high values of 21, 15.2, and 12.8 for CdI$_2$, CdBr$_2$, and CdCl$_2$, respectively, at about 30 eV, indicating strong optical transitions in the intermediate region. The curves of $\varepsilon_{\rm eff}$ saturate at 3, 3.6, and 4 for CdCl$_2$, CdBr$_2$, and CdI$_2$ beyond 20 eV, showing that the contribution of higher-energy transitions is small. The values of $\varepsilon_{\rm eff}(E)$ for large E (Fig. 5) are close to the values of $\varepsilon_1(0)$ reported by Bringans *et al.*[31] who give $\varepsilon_1(0)=3.6$ for CdCl$_2$, $\varepsilon_1(0)=4$ for CdBr$_2$, and $\varepsilon_1(0)=4.6$ for CdI$_2$.

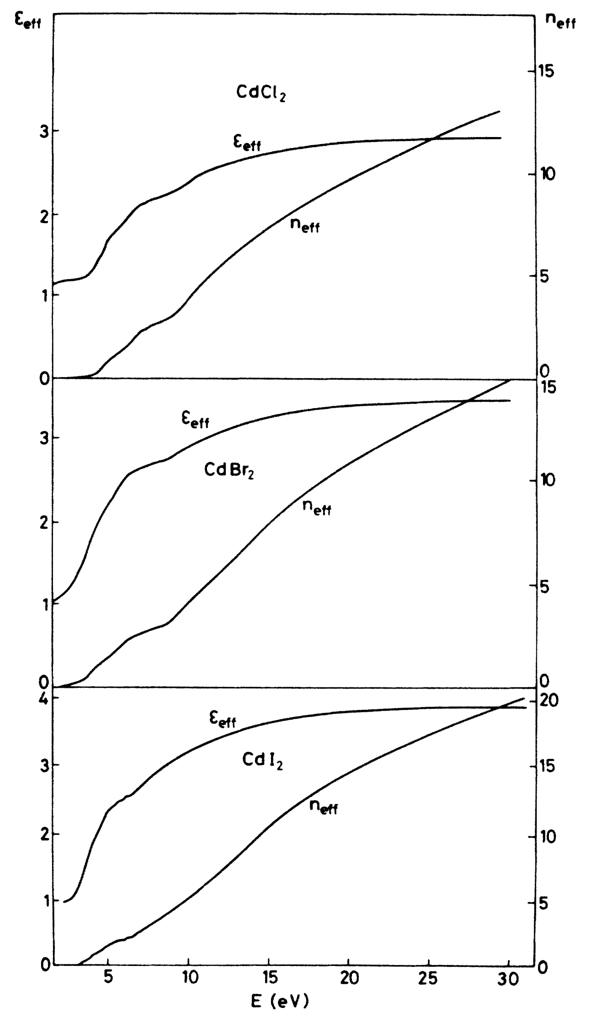

FIG. 5. Values of $n_{\rm eff}(E)$ and $\varepsilon_{\rm eff}$ as a function of E for cadmium halides.

The temperature dependence of the reflectivity in the excitonic region of CdBr$_2$ single crystals is reported in Fig. 6. For peaks A, B, and C a considerable sharpening occurs at low temperature. In particular, the low-energy shoulder of peak B turns into a clear satellite peak below 130–150 K.

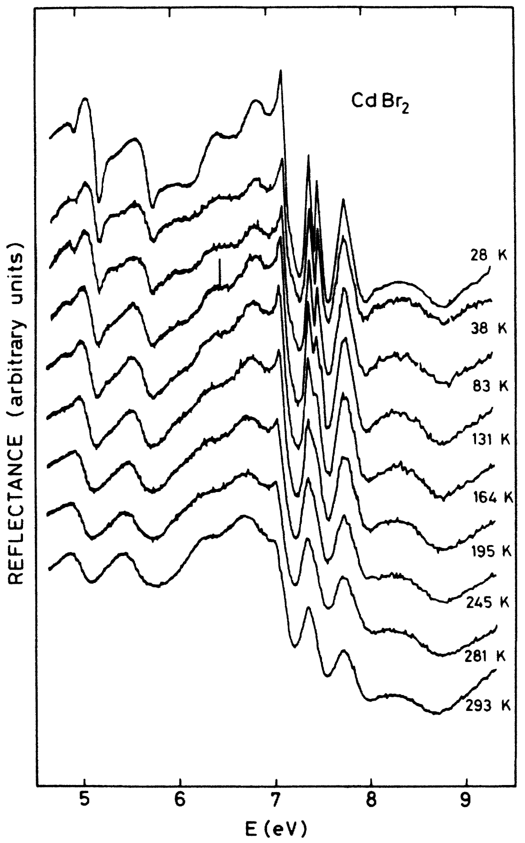

FIG. 6. Temperature dependence of the reflectivity of $CdBr_2$ in the exciton region.

The temperature dependence of the exciton peak positions is shown in Fig. 7. The peak positions can be represented by a formula of the type

$$E(T)=E(0)+B-B\coth(\hbar\omega/2k_BT)\ , \tag{5}$$

where $E(0)+B$ represents the purely electronic excitation energy and B the self-energy of the exciton at $T=0$ due to exciton-phonon interaction. The observed temperature dependence can be described by phonon energies of the order of these observed in infrared reflectivity.[40] However, the data are not sufficiently accurate for a quantitative analysis, because of the width of the peaks at high temperature. The data indicate equal temperature dependences of all peaks, except perhaps for peaks B and C.

Finally, we have compared the reflectivity spectrum of $CdCl_2$ with the soft x-ray absorption spectrum of $CdCl_2$, reported by Sato *et al.*[41] The $Cl(L_{23})$ spectrum of $CdCl_2$ can be divided into three parts: an energy region below 205 eV shows five rather sharp maxima *L*, *M*, *N*, *O*, and *P*; a middle energy region (205 to 209 ev) shows broad absorptions *Q*, *R*, and *S* and a high-energy region beyond 209 eV, with contributions from collective excitations (Fig. 8). We recall that the L_{23} absorption spectrum consists of two components due to spin-orbit interaction of the Cl 2*p* electrons; i.e., the spectrum is a superposition of two similar spectra of different intensity shifted relative to one another by the spin-orbit splitting of 1.6 eV. We

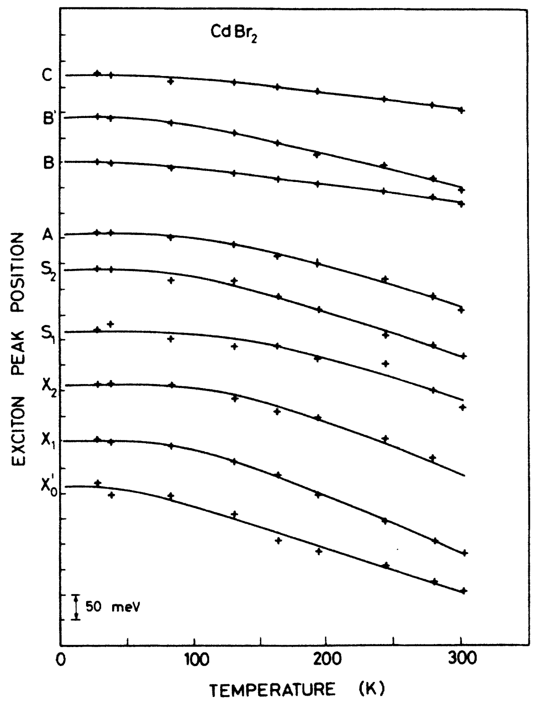

FIG. 7. Temperature dependence of the relative peak position of exciton peaks in $CdBr_2$.

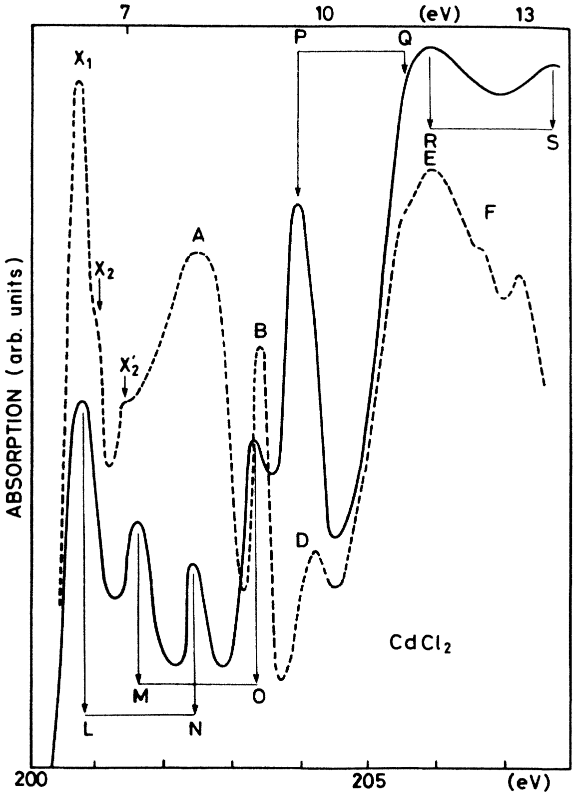

FIG. 8. Comparison between the ultraviolet absorption spectrum (dashed line) obtained from reflection data, and the Cl L_{23} absorption spectrum (solid line) (Ref. 41).

observe some correspondence between the optical and the soft x-ray absorption spectra, as far as the excitation energies are concerned. This suggests that the two types of spectra are due to transitions to common final states of the excited electrons. This is not surprising since the L_{23} shell ($2p$) of Cl and the valence band Cl ($3p$) have the same symmetry.

IV. DISCUSSION

In order to determine the ionic character of the cadmium halides we have applied the dielectric theory of Phillips and van Vechten[42,43] to these materials and have reported the results in Table II. This was part of a general study[44] on the dielectric theory of the chemical bond, applied to crystals with either the $Cd(OH)_2$ or $CdCl_2$ structure, namely the layered Mn, Fe, Co, and Ni dihalides. We obtained values for the ionicity of 0.71 ($CdCl_2$), 0.68 ($CdBr_2$), and 0.66 (CdI_2) in excellent agreement with the values 0.72 ($CdCl_2$), 0.69 $(CdBr)_2$, and 0.67 ($CdCl_2$), deduced by Morioka *et al.*[40] from infrared reflectivity.

The electronic band structure of CdI_2 has been calculated by different authors.[27–30] McCanny *et al.*[27] used a semiempirical tight-binding method and compared the results with angularly averaged and angle-resolved photoemission spectra. Bordas *et al.*[28] have carried out band-structure calculations by means of a linear combination of atomic orbitals (LCAO) and compared their results with optical data. Robertson[29] again used the tight-binding method. Recently Coehoorn *et al.*[30] performed *ab initio* self-consistent relativistic band-structure calculations of the $2H$ and $4H$ polytypes of CdI_2, and compared the calculations with new angle-resolved ultraviolet photoelectric spectroscopy data. The photoelectron spectra show good agreement with the calculated band dispersion.

The calculated band structure of CdI_2 (Fig. 9) shows a band of predominantly I $5s$ character at about 12 eV below the top of the valence band, with a width of 0.8 eV. The Cd $4d$ band is found at 9.9 eV below the top of the valence band. Its total width of 0.8 eV arises from contributions due to spin-orbit coupling and interaction with iodine states. The valence band has mainly I $5p$ character and its calculated width is 4.9 eV. According to the calculations the first conduction band, with a width of 2.6 eV, is at 1.2 eV above the valence band and has mainly Cd $5s$ character. This calculated energy gap of 1.2 eV is too much small as compared to optical data; this is a common error of this type of local-density calculations. Therefore it is necessary to make in CdI_2 a rigid shift of 2.2 eV of the conduction bands relative to the valence bands, in order to obtain agreement between experimental and theoretical direct and indirect gaps. A second conduction band, with mainly Cd $5p$ character, is separated from the first Cd $5s$ type conduction band by a gap of about 1 eV. This second conduction band has states which are strongly hybridized with I $5d$ states. In view of the similarity of the three cadmium halides, one expects the band structures of $CdCl_2$ and $CdBr_2$ to be similar to that of CdI_2.

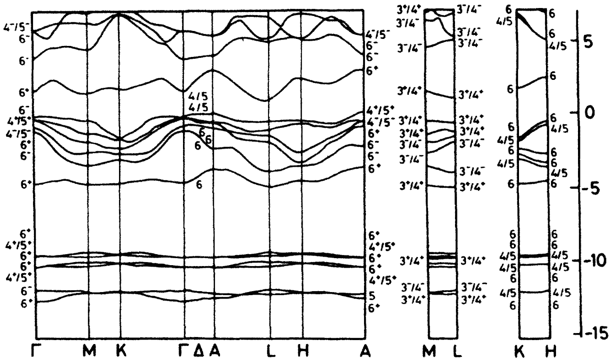

FIG. 9. Band structure of $2H$ CdI_2, including spin-orbit interaction, according to Ref. 30. The conduction bands have been shifted to higher energy by 2.2 eV. The band structure of the $4H$ polytype is very similar.

We also show (in Fig. 10) the band structure of $CdCl_2$ calculated in the same way, i.e., by an *ab initio* self-consistent calculation using the augmented spherical wave (ASW) method, and applying scalar relativistic corrections. For $CdCl_2$, the spin-orbit interaction (which is rather small for the valence and conduction bands) was not taken into account.

We have tried to assign the observed peaks in the optical spectra to specific interband and excitonic transitions. In this assignment we used for CdI_2 the band structure of the $2H$ polytype. Although in most cases the spectra are reported for the $4H$ polytype, the results are not expected

TABLE II. Crystal structures and lattice parameters (crystallographic a and c axes, rhombohedral angle α, crystallographic u parameter) and interatomic distances $d(M\text{-}X)$ and $d(X\text{-}X)$. The Phillips ionicities f_i are calculated, together with the covalent gap E_h and the electronegativity C. The values of the experimental gap E_G^{expt} are compared with the Phillips gap E_G^{Ph}.

Crystal	Types	$CdCl_2(H;R)$ $Cd(OH)_2(H)$ a	c,α	u	$d(M\text{-}X)$ (Å)	$d(X\text{-}X)$ (Å)	E_G^{expt} (eV)	E_g^{Ph} (eV)	C (eV)	E_h (eV)	f_i
$CdCl_2$	H	3.854	19.457	0.25	2.65	3.66	6.6[a]	6.523	5.494	3.51	0.71
	R	6.23	36° 3′								
$CdBr_2$	H	3.954	18.674	0.25	2.76	3.85	5.6[a]	5.61	4.61	3.19	0.68
	R	6.63	34° 0.07′								
CdI_2	H	4.24	6.84	0.25	2.98	4.2	4.3[a]	4.54	3.7	2.63	0.66

[a] R.D. Bringans and W. Y. Liang, J. Phys. C 14, 1065 (1981); experimental values of $\varepsilon_1(0)$ for $CdCl_2$(3.6), $CdBr_2$(4), and CdI_2(4.6) are also reported.

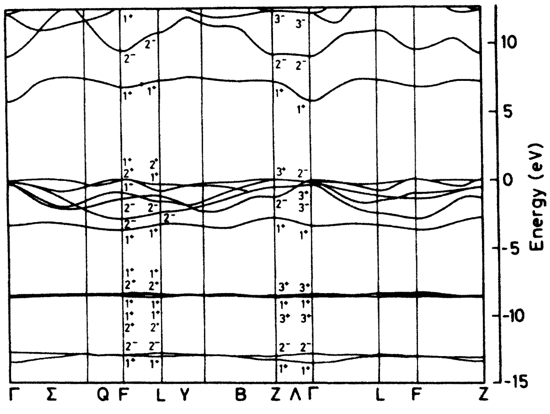

FIG. 10. Band structure of $CdCl_2$, without spin-orbit interaction. The conduction bands have been shifted by 3.2 eV in order to obtain agreement with the observed energy gap.

to be very different, and the transition in the simpler $2H$ structure are easily translated to transitions in the $4H$ polytype. The lower symmetry of $4H$ introduces weak perturbations which do not affect the strong allowed optical transitions discussed in this paper.

We adopted the symmetry notation of Miller and Love for the irreducible representations of the (double) space groups.[45] This notation is different from the notation used in Refs. 8–11: For example representations Γ_5/Γ_6 and Γ_4 in Refs. 8–11 are given by Γ_4/Γ_5 and Γ_6 in our notation. A summary of our assignments is given in Table III.

We assign the peaks X_0, X_1, and X_2 to excitons formed from halogen p-like valence band holes and cadmium $5s$-like conduction-band electrons. According to the calculated band structure of CdI_2, the smallest direct energy gap between the valence band and the Cd $5s$ conduction band occurs at the L point in the Brillouin zone of $2H$-CdI_2, between states $L_3^+/L_4^+ \rightarrow L_3^+/L_4^+$. Optical transitions between these states are parity forbidden, and, as a consequence, these transitions are not expected to give rise to strong excitonic features in the spectra. The first allowed transitions at L are $L_3^-/L_4^- \rightarrow L_3^+/L_4^+$, and occur at an energy of about 1 eV higher. Therefore we ascribe the observed peaks X_0, X_1, and X_2 to exitons associated with the lowest allowed direct transitions, which occur at the Γ point in the Brillouin zone.

The splitting of the states at the top of the valence band at Γ in the cadmium halides can be described in terms of a crystal-field splitting between (p_x,p_y) and p_z states and a spin-orbit parameter. The splitting at Γ has been discussed in terms of such a model, and the nature of the wave functions and intensity of the various possible excitonic transitions can be calculated.[8–11] The results agree quite well with the calculated band structure.[30]

If the spin-orbit coupling is neglected, the transitions at Γ between the valence and the Cd $5s$ conduction band are of the type $\Gamma_2^-(p_z) \rightarrow \Gamma_1^+$ [this is the transition with the lowest energy, because the top of the valence band at Γ has $\Gamma_2^-(p_z)$ character], and $\Gamma_3^-(p_x,p_y) \rightarrow \Gamma_1^+$. The $\Gamma_2^- \rightarrow \Gamma_1^+$ transition is allowed only for polarization of the light with $\mathbf{E} \parallel c$, the $\Gamma_3^- \rightarrow \Gamma_1^+$ transition only for $\mathbf{E} \perp c$. The splitting between Γ_2^- and Γ_3^- states is the crystal-field splitting.

TABLE III. Positions (in eV) and assignments of peaks in the reflectance spectra of cadmium halides at 30 K. Exciton peaks are indicated as (exc), band edges of interband transitions as (band). The assignment of the peak G is tentative.

	$CdCl_2$	$CdBr_2$		CdI_2	
X_0	6.05	4.90	$\Gamma_{6a}^- \rightarrow \Gamma_6^+$ (exc)	3.68	$\Gamma_{6a}^- \rightarrow \Gamma_6^+$ (exc)
X_1	6.36	5.12	$\Gamma_4^-/\Gamma_5^- \rightarrow \Gamma_6^+$ (exc)	3.85	$\Gamma_4^-/\Gamma_5^- \rightarrow \Gamma_6^+$ (exc)
X_1'	6.40	5.40	$\Gamma_4^-/\Gamma_5^- \rightarrow \Gamma_6^-$ (band)	4.30	$\Gamma_4^-/\Gamma_5^- \rightarrow \Gamma_6^+$ (band)
X_2	6.50	5.60	$\Gamma_{6b}^- \rightarrow \Gamma_6^+$ (exc)	4.80	$\Gamma_{6b}^- \rightarrow \Gamma_6^+$ (exc)
X_2'	6.84	6.00	$\Gamma_{6b}^- \rightarrow \Gamma_6^+$ (band)	5.24	$\Gamma_{6b}^- \rightarrow \Gamma_6^+$ (band)
S_1	7.64	6.46	interband Cl $3p$, Br $4p \rightarrow$ Cd $5s$	5.46	interband I $5p \rightarrow$ Cd $5s$
S_2	8.10	6.88			
A	8.39	7.16	$\Gamma_4^+/\Gamma_5^+ \rightarrow \Gamma_6^-$ (exc) or $Z_4^+/Z_5^+ \rightarrow Z_6^-$ (exc)	5.70	$\Gamma_4^+/\Gamma_5^+ \rightarrow \Gamma_6^-$ (exc) or $A_4^+/A_5^+ \rightarrow A_6^-$ (exc)
B	8.82	7.46	excitons Cl $3p$, Br $4p \rightarrow$ Cd $5p$	6.10	$A_{6a}^+ \rightarrow A_6^-$ (exc) or $\Gamma_{6a}^+ \rightarrow \Gamma_6^-$ (exc)
B'		7.62		6.20	
B''				6.44	
C	8.92	7.82		6.70	
C'				7.10	
D	9.64	8.40	interband Cl $3p$, Br $4p \rightarrow$ Cd $5p$	8.10	interband I $5p \rightarrow$ Cd $5p$
D'				8.50	
E	11.80	10.10		9.20	
F	12.70	11.20		10.40	
G	15.80	15.30	Cd($4d$)$\rightarrow$Cd($5p$)?	14.60	

The presence of spin-orbit splitting at Γ gives rise to Γ_6^- and Γ_4^-/Γ_5^- states; the Γ_6^- states are of mixed (p_x,p_y) and p_z character, the Γ_4^-/Γ_5^- are composed of only (p_x,p_y) wave functions. Transitions $\Gamma_4^-/\Gamma_5^-\rightarrow\Gamma_1^+$ are allowed only for $\mathbf{E}\perp\mathbf{C}$, transitions $\Gamma_6^-\rightarrow\Gamma_1^+$ are allowed for both $\mathbf{E}\perp\mathbf{c}$ and $\mathbf{E}\|\mathbf{c}$ polarizations. We assign the X_0 exciton peak in CdI_2 to the direct exciton transition from the highest Γ_6^- state (Γ_{6a}^-) to the Cd 5s conduction-band state Γ_6^+. The exciton peaks X_1 and X_2 are assigned to the transitions $\Gamma_4^-/\Gamma_5^-\rightarrow\Gamma_6^+$ and $\Gamma_{6b}^-\rightarrow\Gamma_6^+$, respectively. Polarization dependent measurements[8–11] show indeed that X_1 occurs only in the $\mathbf{E}\perp\mathbf{c}$, whereas X_0 and X_2 are observed for both $\mathbf{E}\perp\mathbf{c}$ and $\mathbf{E}\|\mathbf{c}$. In the limit of small spin-orbit coupling, the Γ_{6a}^- state has mainly p_z character, and the transition will be strong only for $\mathbf{E}\|\mathbf{c}$. This explains nicely the weak intensity of the X_0 peak in $CdCl_2$, and its increasing intensity in the series $CdCl_2$, $CdBr_2$, and CdI_2 (increasing spin-orbit interaction) for $\mathbf{E}\perp\mathbf{c}$ spectra (Fig. 2). The X_0 exciton peaks in $CdCl_2$ and $CdBr_2$ are much stronger for $\mathbf{E}\|\mathbf{c}$ than for $\mathbf{E}\perp\mathbf{c}$, in agreement with the assignment just given.

The splitting between Γ_4^-/Γ_5^- and Γ_{6b}^- states is largely determined by spin-orbit splitting. Indeed the observed X_1-X_2 splittings (0.14, 0.48, and 0.95 eV for $CdCl_2$, $CdBr_2$, and CdI_2, respectively) are close to the spin-orbit splitting of the atomic p states of the free chlorine, bromine, and iodine atoms (0.116, 0.486, and 1.03 eV, respectively[46]). This supports also our assignment of the X_0, X_1, and X_2 exciton peaks, which is in agreement with the assignment given by Kondo *et al.*[8–11]

The additional features X'_1 and X'_2 are interpreted as the onset of direct allowed interband transitions (corresponding to the excitons X_1 and X_2, respectively). This interpretation leads to values of the optical gap for allowed direct transitions of $E_G=6.40$ eV for $CdCl_2$, $E_G=5.40$ eV for $CdBr_2$, and $E_G=4.30$ eV for CdI_2. The value for CdI_2 is in good agreement with the value of $E_G=4.3$ eV reported by Bringans and Liang.[31] The energy gap of 3.80 eV at 300 K and 4.1 eV at 30 K in CdI_2, reported by Greenaway *et al.*,[2] probably corresponds to the onset of forbidden phonon-assisted direct transitions $L_3^+/L_4^+\rightarrow L_3^+/L_4^+$; the calculated band structure predicts the onset of these transitions at about 0.2 eV below the edge $E_G=4.3$ eV (at 30 K) for allowed direct transitions.

A remarkable feature of the optical spectra of the cadmium halides is that the strong exciton peaks A, B, and C are very sharp, although they occur at several eV above the absorption edge. This is readily explained in terms of the calculated band structure of CdI_2. Because of the gap between the first Cd 5s and the second Cd 5p conduction bands, the excitons A, B, and C fall in a region of little or no background absorption. This is also evident directly from the computed ε_2 versus E curves (Fig. 3): The background absorption ε_2 is low in the region 8–9 eV ($CdCl_2$), 7–8 eV ($CdBr_2$), and 5.5–6.5 eV (CdI_2). The values for CdI_2 agree with the calculated band structure,[30] which predicts a gap between 5.3 and 6.3 eV (after a rigid shift of all conduction bands of 2.2 eV, as mentioned earlier).

The exciton peak A is observed only for $\mathbf{E}\perp\mathbf{c}$ (in $CdCl_2$ and $CdBr_2$), whereas peaks B, B', and C are found in $\mathbf{E}\|\mathbf{c}$ and $\mathbf{E}\perp\mathbf{c}$ spectra.[8–11] The splitting B-B'-C increases strongly from 0.10 eV in $CdCl_2$, 0.36 eV in $CdBr_2$ to 0.6 eV in CdI_2; these values suggest that the splitting is related to the spin-orbit interaction of the halide ion. We assign peak A in CdI_2 to excitons associated with direct transitions $\Gamma_4^+/\Gamma_5^+\rightarrow\Gamma_6^-$ or $A_4^+/A_5^+\rightarrow A_6^-$, allowed only for $\mathbf{E}\perp\mathbf{c}$. The transitions B, B', and C are presumably due to other excitonic transitions between the halide valence band and the Cd 5p conduction band in the region Γ-A, for example, the transitions $\Gamma_{6a}^+\rightarrow\Gamma_6^-$ or $A_{6a}^+\rightarrow A_6^-$. For the rhombohedral structures of $CdCl_2$ and $CdBr_2$, the A peaks are assigned to $\Gamma_4^+/\Gamma_5^+\rightarrow\Gamma_6^-$ or $Z_4^+/Z_5^+\rightarrow Z_6^-$ transitions. The B, B', and C peaks in $CdCl_2$, $CdBr_2$ are due to other transitions between the valence band and the Cd 5p band.

Tentative assignments are also given in Table III for the broad, high-energy structures E to G. Peak G has been assigned to a transition from the Cd 4d to the Cd 5p band;[28,31] however for CdI_2 this assignment does not correspond to the calculated energies.

V. CONCLUSIONS

The interpretation of optical spectra of solids in the region of electronic interband transitions is difficult because of the many possible transitions. A detailed assignment of observed spectral features is usually only possible if extra information about the electronic energy levels is available. In this paper we have shown that a detailed interpretation of the optical reflectance spectrum of CdI_2 is possible, making use of recent self-consistent band-structure calculations. The strong exciton peaks were assigned to direct allowed transitions between the I 5p valence band and the Cd 5s conduction band at the Γ point of the Brillouin zone. The energy gap for these allowed direct transitions is 4.30 eV in CdI_2. However, according to the band-structure calculations, the smallest direct gap is a gap for forbidden transitions between the I 5p band and the Cd 5s band at the L point, with a gap energy $E_G=4.1$ (30 K). The gap for indirect transitions in CdI_2 is between the top of the valence band at A and the minimum of the conduction band at L; the gap energy for these transitions is 3.473 (at 2 K).[7] This identifies three energy gaps for different types of interband transitions in CdI_2.

The reflectance spectra of $CdCl_2$ and $CdBr_2$ are very similar to those of CdI_2. The most important difference is the increasing spin-orbit interaction in the series $CdCl_2$, $CdBr_2$, and CdI_2. This is observed as an increased splitting of some sets of exciton peaks, and is a great help in assigning the peaks. We reported the first band-structure calculation for $CdCl_2$, and compared the observed spectra with the calculations.

A special feature of the spectra of the cadmium halides is the occurrence of very sharp exciton peaks in a spectra region for above the absorption edge. The band structure explains this feature nicely, in terms of an energy gap between the Cd 5s and Cd 5p conduction bands. The large splitting between 5s and 5p states in heavy atoms such as Cd is a scalar relativistic effect (Darwin correction).[47]

ACKNOWLEDGMENTS

We are grateful to A. Lenselink for providing the CdI_2 single crystals used in the reflectance measurements. We also acknowledge the cooperation of our colleague, the late Dr. J. C. Lemonnier, during the early phase of the work. The support of the staff of the "Laboratoire de l'Acceleration Linéaire" de l'Université de Paris-Sud for providing the light beam is acknowledged. One of us (R.C.) was supported by the Netherlands Foundation for Chemical Research (Stichting Scheikundig Onderzoek Nederland), with financial aid from the Netherlands Organization for Advancement of Pure Research (Nederlandse Organisatie von Zuiver-Wetenschappen Onderzoek). The Laboratoire de Spectroscopic at the Université de Rennes I is the "Equipe de Recherche No. 791 associée au Centre National de la Rechereche Scientifigue."

---

[1] G. C. Trigunayat and A. R. Verma, *Crystallography and Crystal Chemistry of Materials with Layered Structures*, edited by F. Levy (Reidel, Dordrecht, 1976), p. 269.

[2] D. L. Greenaway and R. Nitsche, J. Phys. Chem. Solids **26**, 1445 (1965).

[3] D. L. Greenaway and G. Harbeke, Proceedings of the International Conference on Physics of Semiconductors, Kyoto, 1966 [J. Phys. Soc. Jpn. **21**, 251 (1966)].

[4] M. R. Tubbs, J. Phys. Chem. Solids, **29**, 1191 (1968).

[5] M. R. Tubbs, J. Phys. Chem. Solids, **30**, 2323 (1969).

[6] M. R. Tubbs, Phys. Status Solidi **49**, 11 (1972).

[7] Y. Tokemura, T. Komatsu, and Y. Kaifu, Phys. Status Solidi B **72**, K87 (1975).

[8] S. Kondo and H. Matsumoto, Solid State Commun. **24**, 695 (1977).

[9] S. Kondo and H. Matsumoto, J. Phys. Soc. Jpn. **50**, 2379 (1981).

[10] S. Kondo and H. Matsumoto, J. Phys. Soc. Jpn. **51**, 1441 (1982).

[11] H. Matsumoto, H. Nakagawa, and S. Kondo, Mem. Fac. Eng. Fukui Univ. **31**, 53 (1983).

[12] R. M. Yu, J. Phys. Chem. Solids **30**, 63 (1969).

[13] D. K. Wright and M. R. Tubbs, Phys. Status Solidi **37**, 551 (1970).

[14] N. V. Unnikrishnan, H. S. Bhatti, R. D. Singh, G. C. Trigunayat, and S. K. Chaudhary, J. Phys. Chem. Solids **45**, 1205 (1984).

[15] H. Nakagawa, K. Hayashi, and H. Matsumoto, J. Phys. Soc. Jpn. **43**, 1655 (1977).

[16] H. Matsumoto and H. Nakagawa, J. Lumin. **18/19**, 19 (1979).

[17] H. Nakagawa, H. Murata, and H. Matsumoto, J. Lumin. **24/25**, 625 (1981).

[18] T. Hayashi, T. Ohata, and S. Kashino, Solid State Commun. **38**, 845 (1981).

[19] A. B. Lyshkovich, N. K. Gloskovskaja, and I. M. Bolesta, Ukr. Fiz. Zh. **21**, 89 (1976).

[20] A. B. Lyskovich, I. M. Bolesta, and N. K. N. K. Gloskovskaya, Ukr. Fiz. Zh. **21**, 1442 (1976).

[21] A. B. Lyskovich, and M. R. Panasyuk, Ukr. Fiz. Zh. **28**, 135 (1983).

[22] A. Cingolani, M. Ferrara, M. Lugara, and T. Avlijas, Phys. Rev. B **30**, 2229 (1984).

[23] C. Ronda, A. van Heuzen, and C. Haas (unpublished).

[24] M. R. Tubbs, J. Photogr. Sci. **17**, 162 (1969).

[25] J. Malinowski, Photogr. Sci. Eng. **15**, 175 (1971).

[26] E. Inoue, H. Kokado, I. Shimizu, and S. Outsuka, Photogr. Sci. Eng. **17**, 161 (1969).

[27] J. V. McCanny, R. H. Williams, R. B. Murray, and P. C. Kemeny, J. Phys. C **10**, 4255 (1977).

[28] J. Bordas, J. Robertson, and A. Jakobsson, J. Phys. C **11**, 2607 (1978).

[29] J. Robertson, J. Phys. C **12**, 4753 (1979).

[30] R. Coehoorn, G. A. Sawatzky, C. Haas, and R. A. de Groot, Phys. Rev. B **31**, 6739 (1985). See also, R. Coehoorn, Ph.D. thesis, University of Groningen, 1985.

[31] R. D. Bringans and W. Y. Liang, J. Phys. C **14**, 1065 (1981).

[32] J. C. Lemonnier, I. Pollini, J. Thomas, and A. Lenselink, Ann. Isr. Phys. Soc. **6**, 252 (1983).

[33] I. Pollini, J. Thomas, G. Jézequel, J. C. Lemonnier, and A. Lenselink, Phys. Rev. B **29**, 4716 (1984).

[34] F. Levy, Nuovo Cimento **38B**, 359 (1977).

[35] W. Kleber and P. Fricke, Z. Phys. Chem. **224**, 353 (1963).

[36] R. S. Mitchell, Nature **182**, 337 (1958).

[37] I. Pollini, J. Thomas, G. Jézèquel, J. C. Lemonnier, and R. Mamy, Phys. Rev. B **27**, 1303 (1983).

[38] L. Greenaway and G. Harbeke, *Optical Properties and Band Structure of Semiconductors* (Pergamon, New York, 1968).

[39] C. Horie, Progr. Theor. Phys. **21**, 113 (1959).

[40] I. Morioka and I. Nagakawa, Spectrochim. Acta **34A**, 5 (1978).

[41] S. Sato, T. Ishii, I. Nagakura, O. Aita, S. Nakai, M. Yokota, K. Ichikawa, G. Matsuoka, S. Kono, and T. Sagawa, J. Phys. Soc. Jpn. **30**, 459 (1970).

[42] J. C. Phillips, *Covalent Bonding in Crystals, Molecules and Polymers* (University of Chicago Press, Chicago, 1969).

[43] J. C. Phillips, *Bond and Bands in Semiconductors* (Academic, New York, 1973).

[44] J. Thomas and I. Pollini, Phys. Rev. B **32**, 2522 (1985).

[45] S. C. Miller and W. F. Love, *Tables of Irrreducible Representations of Magnetic Space Groups* (Pruett, Boulder, 1967).

[46] C. E. Moore, in *Atomic Energy Levels*, Natl. Bur. Stand. (U.S.) Circ. No. 467 (U.S. G.P.O., Washington, D.C., 1949).

[47] J. C. Slater, *The Quantum Theory of Atomic Structure* (McGraw-Hill, New York, 1960), Vol. II.